

“Anode heel effect” on patient dose in lumbar spine radiography

¹K K L FUNG, MSc, FIR and ²W B GILBOY, PhD, FInstP

¹*Department of Optometry and Radiography, The Hong Kong Polytechnic University, Hung Hom, Kowloon, Hong Kong, China and* ²*Department of Physics, The University of Surrey, Guildford GU2 5XH, UK*

Abstract. Appropriate use of the “anode heel effect” of the output beam from an X-ray tube can reduce the effective dose to patients in some common radiological examinations. We investigated the variation in radiation intensity across the X-ray beam caused by the anode heel effect, and quantified the difference in absorbed dose to critical organs resulting from lumbar spine X-ray projections carried out with the two possible orientations of the patient along the tube axis (cathode to anode). A Rando phantom and some high sensitivity thermoluminescent dosimeters (TLDs) (LiF:Mg,Cu,P) were used. With the tube axis horizontal, radiation intensity profiles, parallel and perpendicular to the axis, were measured. Lumbar spine radiographs were recorded using the Rando phantom in the standard anteroposterior (AP) and lateral projections. TLD pellets were used to measure the absorbed radiation dose at various sites corresponding to critical organ tissues (ovaries, testes, breasts, thyroid and lens). Each set of projections was recorded in two phantom orientations, first with the phantom head placed towards the cathode end of the X-ray tube, and then in the reverse direction. From the radiation intensity profile of the incident X-ray beam, the “cathode end” to “anode end” air dose ratio was found to be 1.8. In lumbar spine radiography, with the phantom head placed towards the anode end of the X-ray tube, the ovaries and testes received an average dose 17% and 12% higher, respectively, in the lateral projection, and 16% and 27% higher, respectively, in the AP projection, than those obtained in the reverse “patient” orientation. These results indicate that patients (particularly females) should always be positioned with the head placed towards the cathode end of the X-ray tube for lumbar spine radiography to achieve significant dose reductions.

Worldwide medical use of ionizing radiation accounts for the great majority of the man-made contribution to average radiation doses. For example, in the United Kingdom, this amounts to 14% (0.37 mSv) of the average annual dose to the population from all sources of radiation [1]. Of the various medical uses of radiation, examination of patients with X-rays for diagnostic purpose is by far the most frequent [2]. The general public are concerned about the harmful effects of ionizing radiation, but radiologists themselves, being in regular contact with radiological equipment, should also be constantly aware of the potential for accruing harmful exposures. The investigation of dose reduction methods in diagnostic radiology has always been a primary aim of radiation protection research. The National Radiological Protection Board (NRPB) in the UK has proposed 28 methods for reducing doses to patients from X-ray examinations, such as using the most sensitive film–screen combination, optimization of

exposures, use of digital imaging equipment and improved procedural techniques [3].

The anode heel effect on the output of X-ray tubes is well documented in radiological physics texts [4–10]. This phenomenon consists of a reduction of X-ray intensity towards the anode side of the X-ray beam, owing to the higher absorption of those X-rays that pass through a greater thickness of material as they emerge from the target. Relative to the centre of the output beam, there may be as many as 25% fewer photons at the anode end of the X-ray tube and 20% more at the cathode end, resulting in a total maximum variation of about 45%; in contrast, there is no significant variation perpendicular to the anode–cathode axis [4]. The anode heel effect is prominent when large field sizes are used at short focal object distances. The effect also increases as the X-ray target angle decreases [5], and with prolonged use of the X-ray tube, owing to pitting of the anode [6]. This effect could produce a discrepancy in optical density of 0.55 on the anode end and 0.84 on the cathode end on a film, with exposure made at 30 in. focal film distance and the collimator opened as wide as possible [7]. The anode heel effect is often

Received 13 July 1999 and in revised form 13 September 1999, accepted 19 October 1999.

deliberately exploited in the radiography of anatomical structures that have large differences in thickness or density. In general, positioning the cathode end of the X-ray tube over the thicker part of the anatomy provides a more uniform radiographic density on the film [8].

In terms of the radiation protection of patients, in some X-ray examinations the anode heel effect may have an implication for dose difference in critical organs or tissues when the patient lying on the X-ray couch is positioned with the head oriented towards either the anode or the cathode end of the X-ray tube. The critical organ doses from X-ray examinations given in NRPB Report 186 are calculated using the Monte Carlo technique, which assumes that the distribution of intensity from the output of the X-ray tube is uniform and ignores the anode heel effect [11].

It is evident that appropriate use of this effect could reduce the dose to critical organs in some common radiological examinations, and the present study was set up to evaluate possible dose differences in critical organs arising from the effect in these two patient orientations. Lumbar spine radiography was selected for this purpose, since this is a very commonly requested X-ray examination, which involves a relatively high patient exposure, with significant dose delivered to the gonads; also, the beam field size along the cathode–anode axis is relatively large, which results in substantial variations in intensity along the body of the patient.

The objectives of this study were: (1) to investigate the radiation intensity variation in the central X-ray beam owing to the anode heel effect along the cathode–anode axis, and along the line perpendicular to this axis; and (2) to quantify the difference in absorbed dose to critical organs and tissues in lumbar spine X-ray projections for the two possible patient orientations along the tube axis. “Critical organs and tissues” include gonads (testes and ovaries), breasts, thyroid and lens of the eyes.

Materials and method

This work was carried out at the X-ray laboratory of the Hong Kong Polytechnic University. A Rando phantom (Radiology Support Devices Inc., Long Beach, CA, USA) was used in this study. This consists of a human skeleton embedded in synthetic tissue-equivalent material forming the natural body contours. It has no limbs and is cut into 36 sequential numbered slices. Each slice contains a regular matrix of holes 5 mm in diameter and 3 cm apart. The holes are normally filled with plugs of the same material, which can be removed and replaced by thermoluminescent dosimeters

(TLDs) for dose measurements at selected locations.

X-ray projections from the phantom were taken with a medium frequency X-ray unit (Toshiba, KXO-30R Minato-ku, Tokyo, Japan), which was installed in 1997. Quality assurance tests for this unit are performed regularly with a non-invasive X-ray test device (4000M Victoreen, Cleveland, OH, USA). These tests include output reproducibility, and tube potential accuracy and reproducibility. Recent results confirmed the very good performance of this X-ray source, with the coefficient of variation for all these tests less than 2%. The collimator was also tested and showed very good alignment with the X-ray beam. Curix (Agfa Gevaert N.V., Mortsel, Belgium) Universal screen/cassettes with Curix XP films were used. An air ionization chamber (MDH 2025 RadCal, Monrovia, CA, USA) with a volume of 3 cm³ was used for radiation intensity profile tests and for calibration of TLDs over the diagnostic range of X-ray energies. This ionization chamber system was annually calibrated by the manufacturer, by a technique traceable to US national standards. Calibration accuracy, energy dependence and repeatability are claimed to be within $\pm 4\%$, $\pm 5\%$ and $\pm 1\%$, respectively.

A TLD reader system (Rialto, NE Technology, Reading, UK) installed in 1994, together with some high sensitivity TLDs of LiF:Mg,Cu,P, were used for dose measurement in critical organ and tissue locations. TLDs were supplied by Harshaw Co. in the form of round sintered disc-shaped pellets 4.5 mm in diameter and 0.8 mm thick. The linearity (dose–response) of these TLDs was tested in previous experiments in the range from a few μGy to a few mGy, and the result showed a good linear fit with the coefficient of determination ($r^2=0.99$). A new batch of these TLDs was initialized by ten cycles of thermal treatment in an oven (Thermolyne Furnace 48000, Thermolyne Co., Dubuque, IA, USA). For each thermal treatment the TLDs were heated to 240°C and maintained at that temperature for 10 min, then cooled to room temperature in a natural draught. Energy response tests for the TLDs were carried out over the diagnostic X-ray energy range of 40–150 kVp using the X-ray unit and the ionization chamber system. The calculated mean response of the TLDs from 40 kVp to 100 kVp was taken as the calibration factor in this study, since in this case the TLDs received X-ray doses mainly from scattered radiation, with the peak voltage set between 80 kVp and 96 kVp for all the projections taken.

The measured air dose was converted to tissue dose using a conversion factor of 1.06; this is the ratio of the mass energy absorption coefficients of tissue and air over the range of photon energies

used [11]. The TLD reader for these high sensitivity TLDs was set to pre-heat at 135°C for 8 s, followed by read-out for 19 s at 240°C and a heating rate of 12°C s⁻¹. This was followed with a machine anneal of 240°C for 90 s. For TLDs that received a high dose from direct beam exposure, the annealing cycle was repeated three times to ensure that the minimum residual dose would be retained from the last exposure. 50 TLDs were selected from the initialized batch, all with homogeneity (sensitivity variation) within 5% of the mean response. The relative sensitivities of these TLDs were determined and their individual calibration factors calculated. Dose readings from these TLDs were estimated to be reliable within $\pm 10\%$ with individual calibration.

Two horizontal profiles of radiation intensity (one along and one perpendicular to the central cathode–anode axis) were measured with the 3 cm³ air ion chamber at 5 cm intervals. Five repeated exposures were made at each location and the mean was recorded. The X-ray beam field size of 52 cm \times 52 cm, measured on the X-ray table, and the focal–object (table) distance of 100 cm were set.

Lumbar spine radiographic projections were performed using the Rando phantom in the standard AP and lateral projections. Dose measurement started when satisfactory radiographs were achieved with good normal collimation and adequate diagnostic film density. TLD pellets were used to measure the absorbed radiation dose at various sites in the phantom corresponding to critical organs or tissues (ovaries, testes, breasts, thyroid and lens). Each location was measured by a group of five TLD pellets and the mean read-out value was recorded. For ovaries, breasts and lens, doses were measured on both the right and left sides. For dose measurement at testes, breasts, thyroid and lens, TLDs were put at the appropriate locations on the surface of the phantom. Each TLD was inserted in a labelled small plastic sachet for individual identification. For dose measurement at the ovary, TLDs were inserted by vacuum tweezers in a sequential order of labelled TLDs at the predetermined ovarian site in slice 29 of the phantom; the choice of this site is based on the fact that the ovary is situated at the level of the iliac spine (interspinous plane) immediately medial to the vertical plane [12] and within the true pelvis against its lateral wall [13].

The whole set of projections was performed in two phantom orientations, first with the phantom head placed towards the cathode end of the X-ray tube, and then in the reverse direction (phantom head towards anode end). Ten exposures were made for each projection to improve the read-out statistics from the TLDs, since, except the ovaries,

all other critical tissues and organs are outside the primary beam. One set of five TLDs was placed on the surface of the phantom at the central beam for entrance skin dose (ESD) measurement. A single exposure was made for entrance skin and ovarian dose measurements.

Results

Tables 1 and 2 show the radiation intensity (air dose) readings at 5 cm intervals along and perpendicular to the central cathode–anode axis, respectively, using an X-ray field size of 52 cm \times 52 cm at the X-ray table surface; these are shown graphically in Figures 1 and 2. From Table 1 and Figure 1, it can be seen that relative to the centre of the field, the air dose increases gradually at the cathode side up to a maximum of +9%, whereas it drops away remarkably towards the anode end of the tube by as much as 55% on the far side of the beam. The data in Table 3 are derived from Table 1 and show that the air dose ratio from cathode end to anode end at the extremities of the beam along the cathode–anode axis was 1.78 for a field length of 40 cm. This ratio drops to 1.12 as the field length decreases to 10 cm. From Table 2 and Figure 2, it can be seen that perpendicular to the cathode–anode axis the air dose profile remains relatively flat throughout, with a very gentle drop on either side of the centre, before falling away more steeply as the field boundaries are approached.

Figure 3 is the radiograph of the pelvis of the phantom, demonstrating the assumed location of the ovary in this study. Figure 4 shows the AP and lateral projections of the lumbar spine of the phantom. Tables 4 and 5 show the radiation dose received by critical organs for the two projections, AP and lateral, of the lumbar spine. Tables 4 and 5 show that, in lumbar spine radiography, with the feet of the phantom placed towards the cathode end of the X-ray tube, the ovaries and testes receive an average dose 16% and 27% higher, respectively, in the AP projection, and 17% and 12% higher, respectively, in the lateral projection, than those obtained in the reverse orientation. In contrast, the mean doses received by the breasts, thyroid and lens were slightly less in both projections when the feet of the phantom faced the cathode end. All the dose differences in both tables are statistically significant ($p < 0.05$) with the paired samples *t*-test using the SPSS statistic software version 7.5 (SPSS Inc., Chicago, IL).

Discussion

Tables 1 and 3 and Figure 1 demonstrate the great variation of X-ray intensity along the

Table 1. Radiation intensity profile (air dose in μGy ($\pm\text{SD}$)) along the central cathode–anode axis in the the X-ray beam of field size of $52\text{ cm} \times 52\text{ cm}$; exposure 80 kVp, 10 mAs

Distance/5 cm interval	Mean air dose (μGy) (from five repeated exposures)	Relative air dose (take centre point as 1)
-8	1 (0)	—
-7	4 (0)	—
-6	3 (0)	—
-5	24 (0)	—
-4	386 (0.5)	0.81
-3	519 (0.7)	1.08
-2	523 (0.5)	1.09
-1	509 (0.5)	1.06
0	479 (0.7)	1
1	454 (0.7)	0.94
2	409 (0.5)	0.85
3	338 (0.5)	0.71
4	216 (0.7)	0.45
5	11 (0)	—
6	4 (0)	—
7	1 (0)	—
8	1 (0)	—

central cathode–anode axis of the X-ray beam. This result is in broad agreement with other published measurements [5, 7–9]. Small variations may be due to the difference in the anode target angle and the age of the X-ray tubes used. Generally speaking, the results show that when the biggest beam field size is used (*e.g.* for abdominal X-ray, using a $43\text{ cm} \times 35\text{ cm}$ film), the X-ray intensity increases gradually in the cathode direction to a maximum of about 9% before dropping rapidly by 19% near the field edge, whereas towards the anode side the intensity

Table 2. Radiation intensity profile (air dose in μGy ($\pm\text{SD}$)) along the line perpendicular to the cathode–anode axis at the centre of the the X-ray beam of field size $52\text{ cm} \times 52\text{ cm}$; exposure 80 kVp, 10 mAs

Distance/5 cm interval	Mean air dose (μGy) (from five repeated exposures)	Relative air dose (take centre point as 1)
-7	3 (0)	—
-6	12 (0)	—
-5	34 (0)	—
-4	387 (0.5)	0.77
-3	479 (0.7)	0.96
-2	490 (0.7)	0.98
-1	502 (0.5)	1.00
0	500 (0.7)	1.00
1	499 (0.5)	1.00
2	495 (0)	0.99
3	484 (0.5)	0.97
4	454 (0.7)	0.91
5	40 (0)	—
6	12 (0)	—
7	6 (0)	—

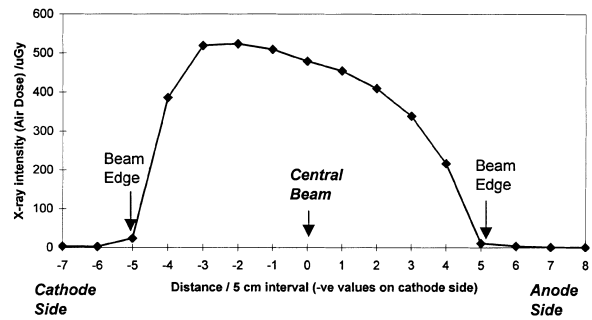


Figure 1. Radiation intensity profile (air dose (μGy)) along the central cathode–anode axis in the X-ray beam of size $52\text{ cm} \times 52\text{ cm}$. Exposure factor 80 kVp, 10 mAs.

declines continuously from the centre of the field, by up to 55% at the field boundary. The derived data in Table 3 give some useful information for the general practice of radiography. Even with an X-ray field length of as little as 10 cm, there is still an X-ray intensity difference of 12% at both edges. This quickly jumps to 27%, 53% and even 78% at beam lengths of 20 cm, 30 cm and 40 cm, respectively, which are commonly used field sizes. If the exposures are made with radiosensitive organs situated nearer to the cathode end of the tube, some avoidable additional radiation will be delivered to those tissues. The level of additional dose will depend on the beam size and the actual amount of exposure given.

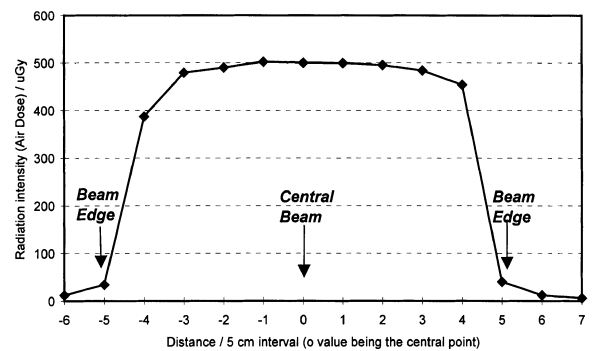


Figure 2. Radiation intensity profile (air dose (μGy)) along the line perpendicular to the cathode–anode axis at the centre of the X-ray beam of field size $52\text{ cm} \times 52\text{ cm}$. Exposure factor 80 kVp, 10 mAs.

Table 3. Comparison of air dose at the edges of the beam with different beam size along the cathode–anode axis (data extrapolated from Table 1); exposure 80 kVp, 10 mAs

Field size along cathode–anode axis (cm)	Air dose ratio, cathode end:anode end
10	1.12
20	1.27
30	1.53
40	1.78

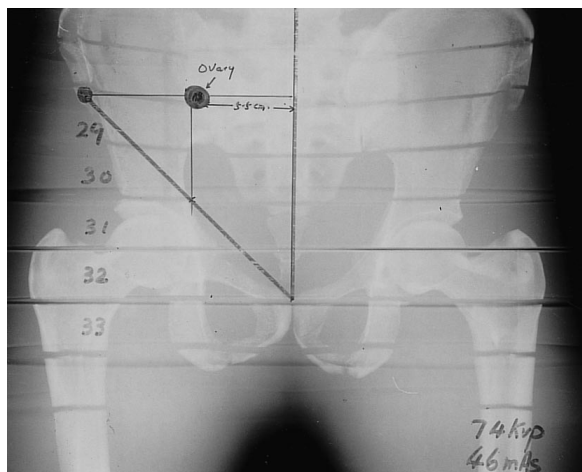


Figure 3. Radiograph of the pelvis of the Rando phantom. The position for the site of the right ovary is indicated in slice 29 of the phantom.

The radiation profile along the line perpendicular to the cathode–anode axis of the central beam is rather flat, with only a very slight gradual drop from the centre to either side. This slight variation has practically no significance in radiography, since the maximum beam width used is seldom greater than 35 cm, as used in radiography of the abdomen.

The ESD and the dose received by various critical organs and tissue in both these projections are similar to previously published figures for mean dose [14]. The use of faster film–screen combinations will definitely lower the overall dose delivered to the patient. Results from Tables 4 and 5 clearly show that in lumbar spine radiography, radiosensitive organs receive higher doses when they are placed near the cathode end of the X-ray tube, owing to the anode heel effect. In lumbar spine radiography, the centre of the X-ray beam passes between the gonads on one side and the breast, thyroid and eyes on the other side, so that with any one of the two projections,

and in whatever cathode–anode orientation, there will always be a situation in which organs on one side receive more dose while at the same time organs on the other side receive less dose. However, when considering organs closer to the central beam, or even within the direct beam, the anode heel effect will have an important impact on the dose distribution. For example, taking lumbar spine radiography of a female patient, data from Tables 4 and 5 show that the ovaries receive 182 μGy and 385 μGy more in the AP and lateral projections, respectively, when the patient's feet are oriented towards the cathode than the doses received in the reverse orientation.

In the same situation, the breasts, thyroid and eyes receive smaller doses, with a total reduction of no more than about 4 μGy in both AP and lateral projections. Furthermore, the ovary is deemed the most radiosensitive organ and has the highest tissue weighting factor of 0.2 in the calculation of effective dose [15]. When considering a male patient for the projections, since the testes are not in the direct beam, it will be noted that the overall effective dose reduction is relatively very low—a few μGy .

The use of high sensitivity TLDs of LiF:Mg,Cu,P (also known as GR200 or TLD100H) enabled us to detect very low dose levels at the positions of some of the critical organs in the phantom. These results indicate that the Rando phantom data could be validated in some degree by placing TLD discs at accessible locations on a real patient. Previous tests in this laboratory showed that these TLDs have a minimum detection limit of 0.6 μGy (at 95% confidence interval) and that phosphor has a sensitivity more than 30 times as great as that of the conventional LiF:Mg,Ti (commonly known as TLD100). Individual calibration for dose measurement in this study improved the detection

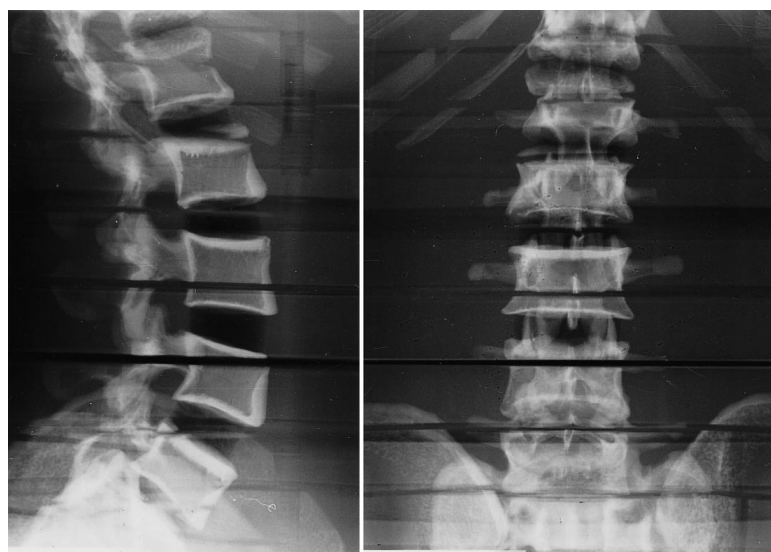


Figure 4. Anteroposterior and lateral projections of the lumbar spine of the Rando phantom.

Table 4. Radiation dose received at critical organs and tissues in anteroposterior projection of the lumbar spine. Exposure 80 kVp, 67.4 mAs; beam field size on skin 14 cm × 24 cm; entrance skin dose 9.06 mGy

Critical organs and tissues	Mean dose (μGy)		Dose difference (μGy) (2)–(1)	% Dose difference
	(1) Feet towards anode	(2) Feet towards cathode		
Ovaries	1147	1329	182	15.9
Testes	20.5	26.1	5.6	27.3
Breasts	53.1	51.9	–1.2	–2.3
Thyroid	6.2	5.5	–0.7	–11.3
Eyes	3.2	3	–0.2	–6.3

Table 5. Radiation dose received at critical organs and tissues in the lateral projection of the lumbar spine. Exposure 96 kVp, 120 mAs; beam field size on skin 11 cm × 20 cm; entrance skin dose 28.81 mGy

Critical organs and tissue	Mean dose (μGy)		Dose difference (μGy) (2)–(1)	% Dose difference
	(1) Feet towards anode	(2) Feet towards cathode		
Ovaries	2259	2644	385	17
Testes	30.5	34.2	3.7	12
Breasts	86	83	–3	–3.5
Thyroid	3.9	3.5	–0.4	–10.3
Eyes	4.8	4.2	–0.6	–12.5

accuracy by a few per cent. 10 exposures for each projection delivered enough dose to these TLDs for good counting statistics at the read-out: for example, the lens received about 40 μGy after 10 exposures of the lateral projection, and each exposed TLD produced around 5000 counts above the background in the thermoluminescent reader, which is usually about 50 counts.

Conclusion

The anode heel effect can be exploited by placing the head of a female patient at the cathode end of the X-ray tube to achieve a significant dose reduction to the ovaries and hence a lower effective dose in lumbar spine radiography. There is a relatively smaller benefit in the dose reduction to the testes for male patients. The thyroid, breast and lens, on the other hand, receive a very small amount of dose increase with this X-ray tube orientation.

Acknowledgment

This research project is funded by the University Research Grant of the Hong Kong Polytechnic University (A/C S-333).

References

1. National Radiological Protection Board (NRPB). Living with radiation London: Stationery Office Publication Centre, 1998:12.

2. United Nations Scientific Committee on the Effects of Atomic Radiation. Sources and effects of ionizing radiation. UNSCEAR 1993 Report. New York: United Nations:228.
3. National Radiological Protection Board. Patient dose reduction in diagnostic radiology, Vol. 1(3). Document of NRPB. London: HMSO, 1990:36–7.
4. Carlton RR, Adler AM. Principles of radiographic imaging: an art and a science. New York: Delmar Publisher Inc., 1992:150–1.
5. Eastman Kodak Co. The fundamentals of radiology. Kodak Publication No. M-18. Rochester, NY: Eastman Kodak, 1980:21–2.
6. Wilks RJ. Principles of radiological physics. Edinburgh: Churchill Livingstone, 1981:285–6.
7. Burns EF. Radiographic imaging: a guide for producing quality radiographs. Philadelphia: WB Saunders Co., 1992:87–91.
8. Curry TS, Dowdery JE, Murry RC. Christensen's physics of diagnostic radiology. Philadelphia, PA: Lea & Febiger, 1990:18–9.
9. Bushong SC. Radiologic science for technologists: physics, biology and protection (6th edn). St Louis: Mosby Year Book, 1997:117–8.
10. Meredith WJ, Massey JB. Fundamental physics of radiology. Bristol: John Wright, 1977:227–9.
11. Jones DG, Wall BF. Organ doses from medical X-ray examinations calculated using Monte Carlo techniques. NRPB Report R186. Chilton: National Radiological Protection Board, 1986:7–8, 17.
12. Makears DW, Owen RH. Surface anatomy for radiographers. Bristol: John Wright, 1980:81.
13. Hamilton WJ. Textbook of human anatomy. Exeter: Macmillan, 1977:435.
14. Plaut S. Radiation protection in the X-ray department. Oxford: Butterworth-Heinemann, 1994:36–7.
15. International Commission on Radiological Protection. Recommendations of the International Commission on Radiological Protection. ICRP Publication 60. Oxford: Pergamon Press, 1991:6.